催化学报
2011 Chinese Journal of Catalysis Vol. 32 No. 3

文章编号: 0253-9837(2011)03-0428-08 国际版 DOI: 10.1016/S1872-2067(10)60183-0 研究论文: 428–435

纳米磁性颗粒负载的银催化剂催化苯乙烯环氧化反应

潘珍燕[1], 华 丽[1], 乔云香[1], 杨汉民[2], 赵秀阁[1], 冯 博[1], 朱闻闻[1], 侯震山[1]

[1]华东理工大学工业催化研究所,结构可控先进功能材料及其制备教育部重点实验室, 上海 200237

[2]中南民族大学催化材料科学湖北省重点实验室, 湖北武汉 430074

摘要: 采用简单浸渍和液相还原法制备了 Ag/KOH-γ-Fe_2O_3 催化剂,并采用 X 射线衍射、透射电镜和 X 射线光电子能谱等方法对催化剂进行了表征. 结果表明,在乙酸乙酯介质中,以叔丁基过氧化氢为氧化剂,该催化剂具有较高的催化苯乙烯环氧化活性, KOH 的添加可大幅度提高环氧化反应活性和选择性. 表征结果显示,反应前后催化剂性质没有发生明显的变化. 另外,所使用的磁性载体有利于负载型银催化剂的分离和循环利用.

关键词: γ-氧化铁; 环氧化; 苯乙烯; 银; 纳米颗粒; 磁分离

中图分类号: O643 **文献标识码**: A

Nanostructured Maghemite-Supported Silver Catalysts for Styrene Epoxidation

PAN Zhenyan[1], HUA Li[1], QIAO Yunxiang[1], YANG Hanmin[2], ZHAO Xiuge[1], FENG Bo[1], ZHU Wenwen[1], HOU Zhenshan[1,*]

[1]*Key Laboratory for Advanced Materials, Research Institute of Industrial Catalysis, East China University of Science and Technology, Shanghai 200237, China*

[2]*Key Laboratory of Catalysis and Materials Science of the State Ethnic Affairs Commission & Ministry of Education, Hubei Province, South-Central University for Nationalities, Wuhan 430074, Hubei, China*

Abstract: The supported silver catalyst Ag/KOH-γ-Fe_2O_3 was prepared by simple impregnation and liquid reduction and then structurally characterized by X-ray diffraction, transmission electron microscopy, and X-ray photoelectron spectroscopy. The supported silver catalysts were highly efficient for the epoxidation of styrene using *tert*-butyl hydroperoxide as the oxidant and ethyl acetate as the reaction medium. The addition of KOH was found to increase the catalytic activity and selectivity significantly. Additionally, the magnetically recoverable γ-Fe_2O_3, as a support, allowed for an easy separation and recycling of the catalyst after the reaction.

Key words: γ-iron oxide; epoxidation; styrene; silver; nanoparticle; magnetic separation

The epoxidation of styrene is of considerable academic and industrial interest. Styrene oxide is a crucial and useful intermediate for fine chemicals and pharmaceuticals [1,2]. Although homogeneous catalysts always have high activity in epoxidation reactions, the conventional homogeneous catalyst systems have serious drawbacks such as catalyst recovery and product separation being very difficult [3,4]. Therefore, catalyst systems with high activity and strong stability are of interest. Additionally, catalysts should be able to be separated and reused easily.

Supported heterogeneous catalysts have separation and recycling advantages compared to homogenous catalysts. Various heterogeneous catalysts have been used for this reaction. Liu et al. [5] studied styrene epoxidation using the Ag-γ-ZrP catalyst with *tert*-butyl hydroperoxide (TBHP) as an oxidant and acetonitrile as the reaction medium, and they achieved a high yield of epoxide (89.8%). Zhang et al. [1] reported that the Ag-Fe_3O_4 nanocomposite gives high activity, selectivity and it is a magnetically separable catalyst after styrene epoxidation with TBHP as oxidant and toluene as solvent. In addition, Co-Y-ZrO_2 [2], Ag/α-Al_2O_3 [6], Au/CNTs [7], Au-HAP [8], CuO/Ga_2O_3 [9], Mn-Ti-Al-

Received 25 October 2010. Accepted 8 December 2010.

***Corresponding author.** Tel: +86-21-64251686; Fax: +86-21-64253372; E-mail: houzhenshan@ecust.edu.cn

Foundation item: Supported by the National Natural Science Foundation of China (20773037, 21073058), the Research Fund for the Doctoral Program of Higher Education of China (20100074110014), and the Key Laboratory of Catalysis and Materials Science of the State Ethnic Affairs Commission and Ministry of Education, Hubei Province, South-Central University for Nationalities (CHCL10001), China.

English edition available online at ScienceDirect (http://www.sciencedirect.com/science/journal/18722067).

MCM-41 [10], and Co/TS-1 [11] catalysts have also been reported and used for styrene epoxidation. Among the reported catalysts, the Ag-based heterogeneous catalysts are especially efficient in the epoxidation reaction.

Iron oxides are environmentally friendly and relatively cheap catalyst supports. There are many different forms of iron oxides such as α-Fe_2O_3, γ-Fe_2O_3, Fe_3O_4, and FeO [12]. Generally, both γ-Fe_2O_3 and Fe_3O_4 have ferromagnetic properties. Nevertheless, γ-Fe_2O_3 as a catalyst support has many advantages. Firstly, γ-Fe_2O_3 is very stable during the reaction while Fe_3O_4 is gradually oxidized to γ-Fe_2O_3 in the presence of an oxidant [13,14]. Secondly, the ferromagnetic property of γ-Fe_2O_3 makes the isolation and recycling of the catalyst more convenient. Although pure γ-Fe_2O_3 often results in low catalytic activity during selective oxidations under mild reaction conditions [3,15], it is very attractive as a magnetically separable catalyst support [16–18].

Although various supported catalysts have been used for styrene epoxidation, previous catalytic systems required toxic organic solvents (toluene, acetonitrile, dichloromethane, 1,2-dichloroethane, and other toxic organic solvents) and, additionally, filtration or centrifugation for the separation of the catalyst. This may result in a mechanic loss of catalyst. In addition, alkali promoters such as K_2CO_3 and $NaHCO_3$ are always added to obtain high activity and selectivity in these oxidation reactions [19,20] but these bases are difficult to reuse and they generate waste after the reaction. To eliminate these problems, a supported-base catalyst has been proposed and used accordingly [21–25]. Therefore, a clean separation and cost effective regeneration of the catalyst and purification of products can be achieved.

We used silver as a catalytically active component and then prepared a heterogeneous epoxidation catalyst by combining the advantages of a magnetic support with a supported-base promoter. In the first step, the magnetic γ-Fe_2O_3 nanoparticles were modified by solid base KOH and then silver was immobilized on the base-modified magnetic support by simple impregnation and consequent liquid reduction. Subsequently, styrene epoxidation was carried out over the prepared magnetic catalyst with low toxic ethyl acetate as the reaction solvent. We found that the as-obtained catalyst was very efficient for styrene epoxidation. Finally, the recyclability of the ferromagnetic nanocatalyst was also examined.

1 Experimental

1.1 Preparation of the catalysts

1.1.1 Preparation of magnetic γ-Fe_2O_3 particles

$FeCl_3·6H_2O$ (5.00 g, 18.5 mmol, Sinopharm Chemical Reagent Co., Ltd., Shanghai (SCRC), AR grade) and $(NH_4)_2SO_4·FeSO_4·6H_2O$ (5.44 g, 13.9 mmol, SCRC, AR grade) were dissolved in 200 ml of distilled water in a beaker. $NH_3·H_2O$ (SCRC, AR grade) was then rapidly added to the mixture under nitrogen and the pH of the solution was adjusted to above 9. The whole mixture was stirred at 30 °C for a further 2 h. The products were black precipitates. After 3 h of aging the black precipitates were washed with water and alcohol several times and subsequently dried at 80 °C for 6 h followed by calcination at 300 °C for 2 h.

1.1.2 Preparation of KOH-γ-Fe_2O_3

γ-Fe_2O_3 (2.00 g) was impregnated with KOH (0.008 g, SCRC, AR grade), dissolved in 1 ml of distilled water in a beaker and then stirred at room temperature for 24 h. Afterwards, the mixture was dried under vacuum at 80 °C for 2 h followed by calcination at 300 °C for 2 h. Catalysts with different KOH loadings were also prepared.

1.1.3 Preparation of 10%Ag/0.4%KOH-γ-Fe_2O_3

KOH-γ-Fe_2O_3 (0.200 g), polyvinylpyrrolidone (PVP, 0.100 g, SCRC, AR grade), and $AgNO_3$ (0.032 g, (SCRC, AR grade) were dispersed in 1 ml of distilled water in a beaker. The mixture was stirred at 80 °C for 8 h until all the silver ions in the solution were adsorbed onto the support (No residual silver ions were detected in the aqueous phase by the sodium chloride (SCRC, AR grade) test. Cooling the solution to 0 °C, a $NaBH_4$ (0.5 mol/L, 2 ml, SCRC, AR grade) aqueous solution was added to the mixture and stirred for 1 h. The materials were then washed three times with distilled water and ethanol. The washed catalyst particles were dried under vacuum at 80 °C for 2 h followed by aging for 3 h at 80 °C under nitrogen. The content of potassium hydroxide in the catalyst was about 0.4% as determined by ICP-AES, which confirms that the loss of potassium hydroxide was negligible during catalyst preparation. The preparation of the magnetically recoverable catalysts Ag/KOH-γ-Fe_2O_3 is shown in Scheme 1.

1.2 Characterization of the catalysts

The X-ray diffraction (XRD) pattern of the catalysts was analyzed by powder XRD D/max 2550 VB/PC using Cu $K_{\alpha 1}$ radiation (λ = 0.154056 nm). The sample was scanned over a 2θ range from 10° to 80° at a scanning rate of 0.02°/s. Transmission electron microscopy (TEM) was performed with a JEOL JEM 2100T HRTEM instrument operating at 200 kV. X-ray photoelectron spectroscopy (XPS) measurements were performed on a Thermo ESCALAB 250 spectrometer using Nonmonochro Al K_α radiation. The binding

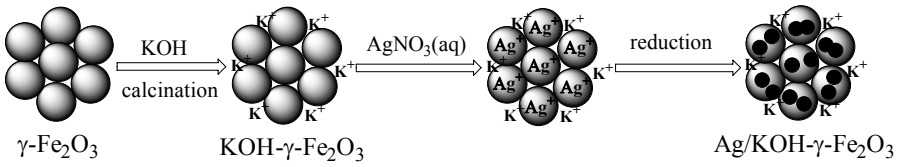

Scheme 1. Synthetic route for the magnetically recoverable catalyst Ag/KOH-γ-Fe_2O_3.

energies were calibrated with the C 1*s* level of adventitious carbon (284.8 eV) as the internal standard. The Ag and K contents were analyzed by ICP-AES analysis on a Varian 710-ES instrument. A Thermo Nicolet Nexus 670 was used for FT-IR characterization.

1.3 Catalytic tests

The catalyst (0.020 g), styrene (0.104 g, 1 mmol, Shanghai Ling Feng Chemical Reagent Co., Ltd., AR grade), and ethyl acetate (1.792 g, 2 ml, SCRC, AR grade) were placed in a 25 ml Schlenk glass flask under a N_2 atmosphere and then stirred at room temperature for 30 min. TBHP (0.390 g, 3 mmol, SCRC, AR grade) was added to the reaction mixture, which then proceeded for the required time at 80 °C. After the reaction the catalyst was separated simply by a magnet and washed with ethyl acetate followed by drying in vacuum. The catalyst was then conveniently used for a next run. The reaction products were analyzed by gas chromatography using an FID detector.

2 Results and discussion

2.1 Characterization results

The formation of metallic Ag and γ-Fe_2O_3 in the Ag/KOH-γ-Fe_2O_3 catalyst was confirmed by powder XRD (Fig. 1). A single phase of γ-Fe_2O_3 was prepared successfully. The XRD pattern of the catalyst (Fig. 1(1)) shows that the peaks matched well with standard γ-Fe_2O_3 reflections (JCPDS 25-1402). Figure 1(2) shows the XRD pattern of the 10%Ag/0.4%KOH-γ-Fe_2O_3 composite. Apart from the characteristic diffraction peaks of the γ-Fe_2O_3 reflections the clear diffraction peaks at 2θ = 38.12°, 44.26°, 64.48°, and 77.36° are assigned to the (111), (200), (220), and (311) crystal planes of silver, respectively. These are in good agreement with the standard Ag(0) reflections (JCPDS 65-2871). Figure 1(3) shows the XRD pattern of the 10%Ag/0.4%KOH-γ-Fe_2O_3 composites after five runs. There was not much change in the XRD pattern compared to the fresh catalyst. The lower iron oxide diffraction was most likely due to the low crystallinity of iron oxide and the heavy atom effect arising from the silver atoms [26].

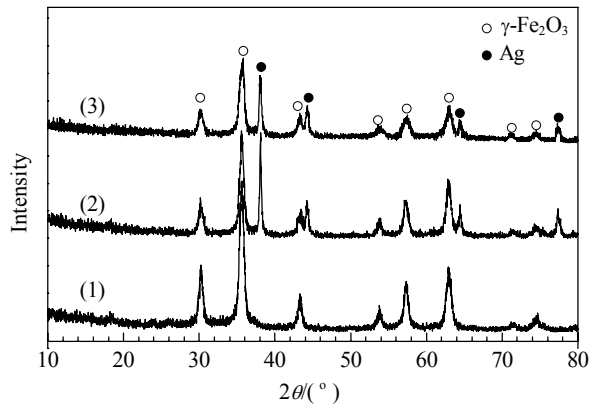

Fig. 1. XRD patterns of γ-Fe_2O_3 (1), 10%Ag/0.4%KOH-γ-Fe_2O_3 before (2) and after five runs (3).

Figure 2 shows TEM photographs and the size distribution of the fresh and reused nanoparticles. The nanocomposites consisted of nearly spherical nanoparticles with an average diameter of 7–9 nm. The overall shape and size distribution of the particles did not show obvious changes even after five runs for the magnetically separable nanocatalyst.

The surface composition and oxidation state of the nanocatalyst were also analyzed by XPS. Figure 3 shows representative XPS spectra of the nanocatalyst. Elemental analysis confirmed the presence of Ag, Fe, K, C, and O. The observed XPS spectra of C 1*s* (284.8 eV) and O 1*s* (530.4 eV) came from adventitious carbon and iron oxides. In addition, a relatively weak Fe 3*p* line at 56.1 eV was also detected (Fig. 3). No other metallic signals were detected in the XPS spectra.

Figure 4 shows the Fe 2*p* spectra of the different samples. All the Fe 2*p* spectra show a typical iron oxide structure with broad main peaks (Fe $2p_{3/2}$ and Fe $2p_{1/2}$). The characteristic doublet of Fe $2p_{3/2}$ and $2p_{1/2}$ were observed as photoelectron peaks at 710.5 and 724.1 eV, respectively. The Fe 2*p* data were in good agreement with the values reported for γ-Fe_2O_3 in the literature [27,28]. These spectra show that the Fe 2*p* signal intensity and binding energy of composites (1) and (2) remained unchanged. After reusing Ag/KOH-γ-Fe_2O_3 five times there was also no remarkable change in the Fe 2*p* peak intensity or the binding energy (Fig. 4(3)). These results show that the addition of KOH or Ag did not affect the structure of γ-Fe_2O_3 and γ-Fe_2O_3 was very stable during catalytic recycling.

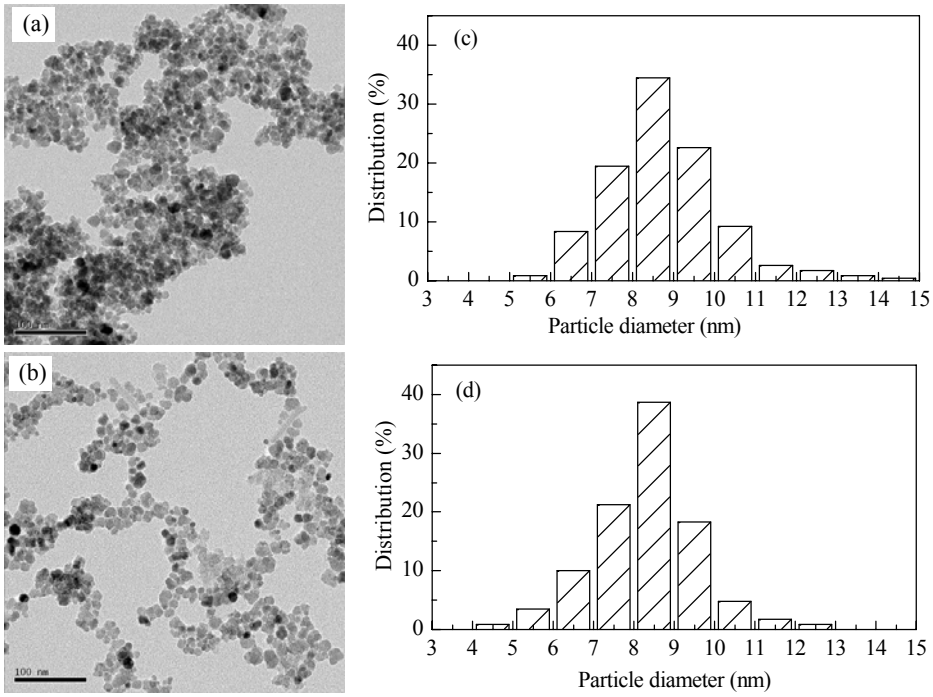

Fig. 2. TEM images (a and b) and particle size distribution (c and d) of 10%Ag/0.4%KOH-γ-Fe_2O_3 before (a and c) and after five runs (b and d).

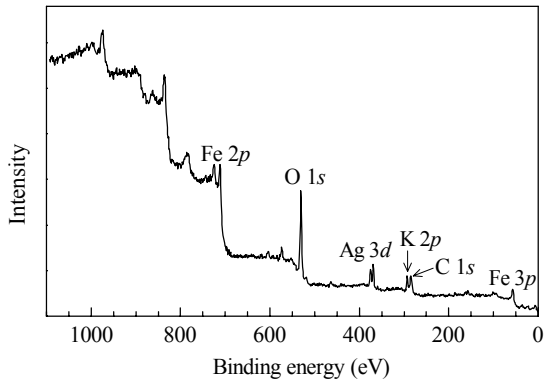

Fig. 3. The XPS spectrum of the 10%Ag/0.4%KOH-γ-Fe_2O_3 composite.

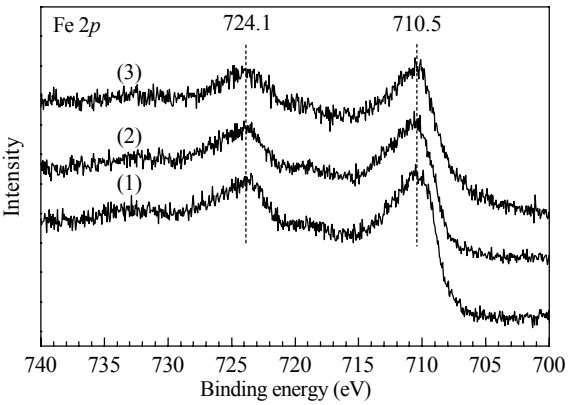

Fig. 4. Representative Fe 2*p* XPS spectra of the composites. (1) Ag/γ-Fe_2O_3; (2) 10%Ag/0.4%KOH-γ-Fe_2O_3; (3) 10%Ag/0.4%KOH-γ-Fe_2O_3 after five runs.

To determine the oxidation state of the Ag component the XPS technique was used. Figure 5 shows the Ag 3*d* spectra of different samples and this could be resolved into two spin orbit components, Ag $3d_{5/2}$ and Ag $3d_{3/2}$. Figure 5(a) gives the XPS signal of the catalyst Ag_2O/ KOH-γ-Fe_2O_3, which was not pre-reduced by $NaBH_4$, and the main peak for Ag $3d_{5/2}$ was present at a binding energy of 367.84 eV. This was close to the values of Ag^+ in Ag_2O [29,30]. Figure 5(b) shows the XPS spectrum of the freshly reduced Ag/KOH-γ-Fe_2O_3 catalyst and the main peaks (Ag $3d_{5/2}$) are present at binding energies of 368.09 and 367.60 eV, respectively. This data indicates that the reduced catalyst contained a higher amount of metallic silver and less ionic silver in Ag_2O [31–33]. The XRD data (Fig. 1(2)) did not indicate the presence of Ag_2O but the XPS results did indicate the possible existence of a few atomic layers of Ag^+ species on the nanoparticle surfaces [34]. Figure 5(c) shows the XPS spectrum of the Ag/KOH-γ-Fe_2O_3 catalyst after five runs and the main peaks (Ag $3d_{5/2}$) were present at binding energies of 368.26 and 367.79 eV. Although the XPS results show that a small amount of Ag_2O was still present on the surface of the nanocatalyst the XRD data (Fig. 1(3)) showed that Ag_2O was not present on the surface of the nanocatalyst. Additionally, the main peak at 368.26 eV (Ag $3d_{5/2}$) for the recycled catalyst shifted 0.17 eV higher in terms of binding energy compared to the fresh catalyst. Because a more positive charge density on typical transition metal atoms results in higher binding energies, the Ag nanoparticles were more positive after five runs, which

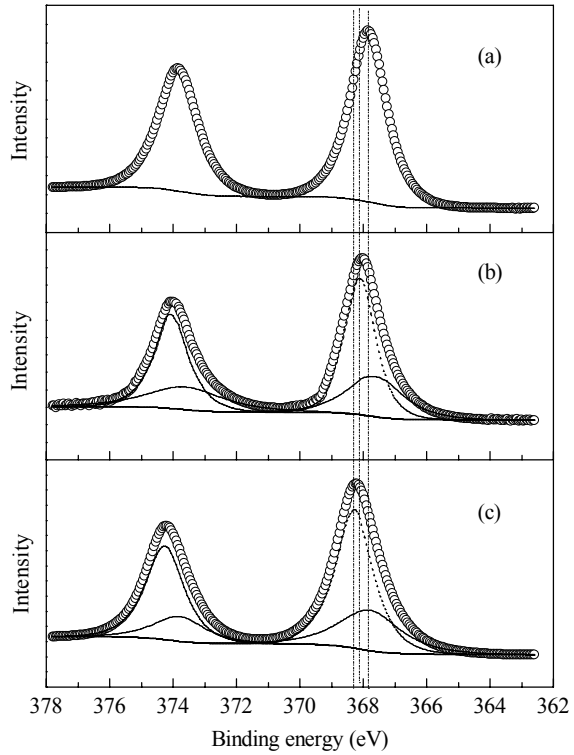

Fig. 5. Representative Ag 3*d* XPS spectra of the nanocomposites. (a) The catalyst was not reduced by $NaBH_4$; (b) 10%Ag/0.4%KOH-γ-Fe_2O_3; (c) 10%Ag/0.4%KOH-γ-Fe_2O_3 after five runs.

might be due to the oxidant in the reaction system.

The detailed XPS parameters of all the samples are summarized in Table 1. The XPS spectra also contained a K 2*p* signal and the K $2p_{3/2}$ peak was present at a binding energy of 292 eV [35,36]. The peak intensity and binding energy of the K 2*p* peak did not change after these reactions (Table 1).

Table 1 XPS results of the catalysts

Catalyst	Binding energy (eV)		
	Ag $3d_{5/2}$	Fe $2p_{3/2}$	K $2p_{3/2}$
Ag_2O/0.4%KOH-γ-Fe_2O_3[a,b]	367.84	710.43	292.20
Ag/0.4%KOH-γ-Fe_2O_3[b]	367.60	710.48	292.15
	368.09		
Ag/0.39%KOH-γ-Fe_2O_3[b,c]	367.79	710.46	292.20
	368.26		

[a]The unreduced catalyst was used.

[b]The potassium hydroxide content was determined by ICP-AES.

[c]10%Ag/0.4%KOH-γ-Fe_2O_3 was recycled five times.

2.2 Catalytic activity for epoxidation with the magnetic silver catalyst

The transformation of styrene to styrene oxide (SO) upon catalysis by the γ-Fe_2O_3, KOH-γ-Fe_2O_3, Ag/γ-Fe_2O_3, and Ag/KOH-γ-Fe_2O_3 catalysts was investigated and the results are listed in Table 2. We found that only benzaldehyde (BZ) was formed as a main by-product. The content of Ag in the Ag/KOH-γ-Fe_2O_3 catalyst has been optimized and we show that a catalyst loading of 10% Ag gives the most active catalyst. Therefore, catalysts loaded with 10% Ag were used in the following studies.

When single γ-Fe_2O_3 was used as the catalyst the selectivity for SO and BZ was 47.8% and 52.2%, respectively (Table 2, entry 2). The selectivity for SO was improved to 81.9% when using the 10%Ag/γ-Fe_2O_3 catalyst (Table 2, entry 4), which confirmed clearly that both Ag and γ-Fe_2O_3 components played a synergic role in the catalytic epoxidation. It has been reported previously that γ-Fe_2O_3 provides reactive oxygen species [37,38] and the active species may easily transfer to the surface of the proximate Ag particles in the nanocatalyst. As a consequence, this process facilitated the epoxidation of the styrene molecules adsorbed on the Ag surface. Styrene epoxidation gave a very low conversion (16.4%) in the absence of a catalyst (Table 2, entry 1), which demonstrates the necessity for a catalyst in this system.

Table 2 Epoxidation of styrene with different catalysts in ethyl acetate

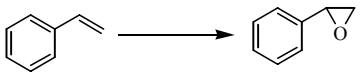

Entry	Catalyst	Conversion (%)	Selectivity (mol%)	
			SO	BZ
1	None	16.4	41.8	58.2
2	γ-Fe_2O_3	80.7	47.8	52.2
3[a]	0.4%KOH-γ-Fe_2O_3	78.5	53.6	46.4
4	10%Ag/γ-Fe_2O_3	70.0	81.9	18.1
5[a]	10%Ag/0.1%KOH-γ-Fe_2O_3	79.9	83.0	17.0
6[a]	10%Ag/0.4%KOH-γ-Fe_2O_3	89.6	89.7	10.3
7[a]	10%Ag/0.91%KOH-γ-Fe_2O	75.5	82.7	17.3

Reaction conditions: styrene 1 mmol, catalyst 20 mg Ag 18.5 μmol, ethyl acetate 1.792 g (2 ml), TBHP 3 mmol, 80 ºC, 15 h, N_2 atmosphere. Conversion and selectivity were determined by GC analysis.

[a]The contents of potassium hydroxide were determined by ICP-AES.

2.2.1 Effect of K loading

The effects of different KOH loadings on the conversion of styrene and the selectivity for SO were also examined (Table 2, entries 5–7). When 0.4%KOH/γ-Fe_2O_3 was used as the catalyst, the selectivities for SO and BZ were 53.6% and 46.4%, respectively (Table 2, entry 3). Obviously, the γ-Fe_2O_3 modified by a solid base KOH improved the selectivity for SO. Moreover, it can be seen that with an increase in the amount of KOH loading in the supported-silver catalyst both the conversion of styrene and the selectivity for SO increased correspondingly and a maximum was found for 0.4% KOH (Table 2, entries 5 and 6). However, when the supported amounts of KOH exceeded 0.4%, the conversion and selectivity dropped to 75.5% and 82.7% (Table 2,

entry 7), respectively.

2.2.2 Effect of solvents

As shown in Table 3, the epoxidation of styrene in different media was investigated. It was clear that the properties of the solvents greatly affected the conversion and selectivity. Benzoic acid (BA) was the main product obtained under solvent-free conditions after a 15 h reaction (Table 3, entry 2). The selectivity for SO, BZ, and BA is almost the same (36.4%, 30.9%, and 32.7%, respectively) with a reaction time of 7 h (Table 3, entry 1). This implied that SO and BZ can be further oxidized to BA possibly because of the high local concentration of SO, BZ, and TBHP around the catalyst under solvent-free conditions. When the reaction was performed in an aqueous medium, with an increase in the reaction time the selectivity for SO decreased while that for the aldehyde increased (not shown). After a 15 h reaction time, BZ was the main product with a moderate conversion (Table 3, entry 3). The change in selectivity for BA and phenylethylene glycol was found to be quite small. The observed variation in product selectivity suggests that SO undergoes C–C bond breakage to produce BZ as the main product in the water medium. Solvents like ethanol (SCRC, AR grade), ethyl acetate, and acetonitrile (Shanghai Ling Feng Chemical Reagent Co., Ltd., AR grade) (Table 3, entries 4–6) are more favorable for the formation of SO. The conversion of styrene in ethyl acetate and acetonitrile was higher and reached 89.6% and 90.5%, respectively. Because ethyl acetate is a more environmentally benign solvent it was used as a reaction medium in the following catalytic reactions.

Table 3 Epoxidation of styrene with the 10%Ag/0.4%KOH-γ-Fe_2O_3 catalyst in different solvents

Entry	Solvent	Conversion (%)	Selectivity (mol%)			
			SO	BZ	BA	Enol
1[a]	none	48.6	36.4	30.9	32.7	0
2	none	74.1	4.8	10.3	84.9	0
3	water	47.8	12.1	72.9	12.5	2.4
4	ethanol	37.9	85.6	14.4	0	0
5	ethyl acetate	89.6	89.7	10.3	0	0
6	acetonitrile	90.5	89.6	10.4	0	0

Reaction conditions: styrene 1 mmol, catalyst 20 mg (Ag 18.5 μmol), solvent 2 ml, TBHP 3 mmol, 80 ºC, 15 h ([a]7 h), N_2 atmosphere. Conversion and selectivity were determined by GC analysis.

2.2.3 Reaction kinetics and catalyst recycling

The catalytic performance of the epoxidation of styrene versus reaction time was studied and this is shown in Fig. 6. The conversion of styrene increased continuously with time and was close to full conversion after 24 h. The yield of styrene epoxide was comparable with many of the heterogeneous catalytic systems reported earlier, even in other organic solvents [39,40]. Interestingly, both the selectivity for SO (ca. 89%) and BZ (ca. 10%) were low and constant during the whole process. This data shows that the SO and BZ were formed simultaneously in the reaction. The selectivity for SO was quite high and the formation of BZ or BA was suppressed considerably in ethyl acetate compared with that in aqueous medium or without the use of a solvent. Our proposed reaction mechanism is shown in Scheme 2.

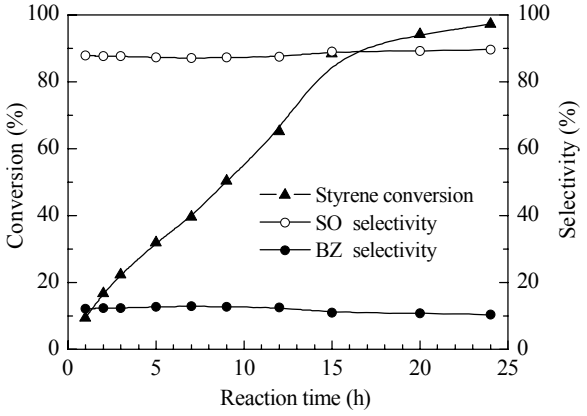

Fig. 6. Catalytic performance of the 10%Ag/0.4%KOH-γ-Fe_2O_3 catalyst as a function of reaction time. Reaction conditions: styrene 1 mmol, catalyst 20 mg (Ag 18.5 μmol), ethyl acetate 1.792 g (2 ml), TBHP 3 mmol, 80 ºC, N_2 atmosphere.

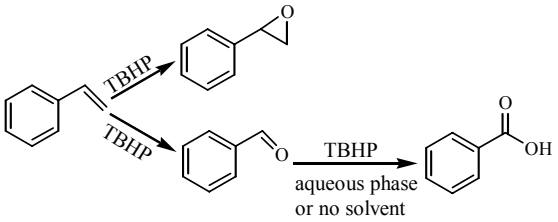

Scheme 2. Reaction scheme for the epoxidation of styrene.

Recycling experiments were also undertaken for the epoxidation of styrene using the Ag/KOH-γ-Fe_2O_3 catalyst (Fig. 7). After the first reaction, the catalyst was recovered easily using a permanent magnet and the products were simply collected by decantation. The recovered catalyst was then washed with ethyl acetate (1 ml × 3) and dried under vacuum. The catalyst was reused in successive epoxidations by the addition of fresh solvent, TBHP, and substrate. The catalytic system gave 89.6% conversion for the second run and 80.1% conversion for the fifth run. Because the charge density, the overall shape and the size distribution of the catalytically active silver nanoparticles did not change significantly after consecutive runs as discussed above a gradual decrease in the conversion of styrene occurred. This was possibly because of the dissolution of silver or potassium

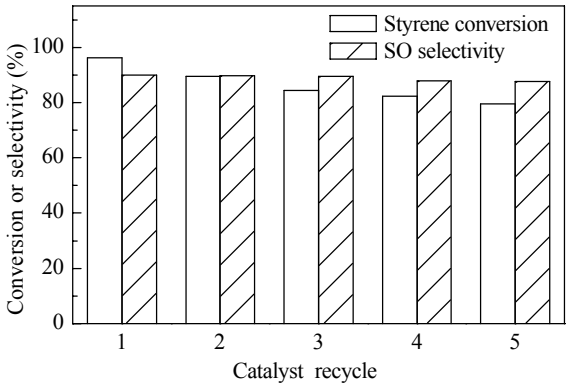

Fig. 7. Reuse of the 10%Ag/0.4%KOH-γ-Fe_2O_3 catalyst for the epoxidation of styrene. Reaction conditions: styrene 1 mmol, catalyst 20 mg (Ag 18.5 μmol), ethyl acetate 1.792 g (2 ml), TBHP 3 mmol, 80 ºC, 24 h, N_2 atmosphere.

leaching into the reaction mixture, especially in the liquid phase oxidation reactions. To address this possibility, the isolated products obtained after magnetic separation were analyzed by ICP-AES. We found that the Ag concentration in the reaction effluent was only 0.3×10^{-6} and the content of KOH in the reused Ag/KOH-γ-Fe_2O_3 catalyst remained unchanged (0.39%). This indicates that the leaching of Ag or K during the reaction was negligible. Based on the analysis above, the strong adsorption of the reaction products onto the surface of the catalyst could be the reason for the slow deactivation in the catalytic runs. This is also shown by the C–H stretching bands (2961.2 and 2926.7 cm^{-1}) present in the IR spectra of the reused catalyst by comparison with the fresh catalyst. Because of the high affinity of Ag and KOH for the magnetic support, a highly efficient magnetic separation can be achieved for this catalytic system.

2.2.4 Epoxidation reaction of different substrates

In the next step, the generality of the oxidative reaction was investigated by varying the alkene substrates and comparing their conversions and product selectivities as listed in Table 4. The 10%Ag/0.4%KOH-γ-Fe_2O_3 catalyst showed much higher activity for styrene than the cycloolefins and the linear alkene. The styrene, cyclooctene (Alfa Aesar, AR grade), and 1-octene (Alfa Aesar, AR grade) were converted into corresponding epoxides with excellent selectivity (Table 4, entries 1, 3, and 4) but the oxidation of cyclohexene (SCRC, AR grade) resulted in the production of enols (Table 4, entry 2).

Table 4 Epoxidation of various substrates with the 10%Ag/0.4%KOH-γ-Fe_2O_3 catalyst in ethyl acetate

Entry	Substrate	Conversion (%)	Selectivity (mol%)		
			Epoxides	Aldehyde	Enols
1	styrene	89.6	89.7	10.3	—
2	cyclohexene	26.6	30.1	—	69.9
3	cyclooctene	28.5	91.4	—	8.6
4	1-octene	14.2	93.8	—	6.2

Reaction conditions: substrate 1 mmol, catalyst 20 mg (Ag 18.5 μmol), ethyl acetate 1.792 g (2 ml), TBHP 3 mmol, 80 °C, 15 h, N_2 atmosphere. Conversion and selectivity were determined by GC analysis.

3 Conclusions

A supported silver catalyst was successfully prepared by the reduction of silver salts and they were supported on the magnetically recoverable γ-Fe_2O_3. The magnetically recyclable catalyst system was highly efficient in catalyzing the epoxidation of styrene with ethyl acetate as the reaction medium. The reduced metallic Ag component and the supported-base promoter played important roles in improving activity and selectivity during styrene epoxidation. Obviously, this catalyst system is green, simple, easily separable, and recyclable.

Acknowledgments

The authors would like to express their thanks to Prof. Walter Leitner for the helpful suggestion and Dr. Nils Theyssen for assistance.

References

1 Zhang D H, Li G D, Li J X, Chen J S. *Chem Commun*, 2008: 3414
2 Tyagi B, Shaik B, Bajaj H C. *Catal Commun*, 2009, **11**: 114
3 Garade A C, Bharadwaj M, Bhagwat S V, Athawale A A, Rode C V. *Catal Commun*, 2009, **10**: 485
4 Dioumaev V K, Bullock R M. *Nature*, 2003, **424**: 530
5 Liu J H, Wang F, Gu Z G, Xu X L. *Catal Commun*, 2009, **10**: 868
6 Chimentão R J, Kirm I, Medina F, Rodríguez X, Cesteros Y, Salagre P, Sueiras J E, Fierro J L G. *Appl Surf Sci*, 2005, **252**: 793
7 Liu J H, Wang F, Xu T, Gu Z G. *Catal Lett*, 2010, **134**: 51
8 Liu Y M, Tsunoyama H, Akita T, Tsukuda T. *Chem Commun*, 2010, **46**: 550
9 Choudhary V R, Jha R, Chaudhari N K, Jana P. *Catal Commun*, 2007, **8**: 1556
10 王广健, 刘正旺, 刘义武, 刘广卿, 徐明霞, 王 磊. 催化学报(Wang G J, Liu Zh W, Liu Y W, Liu G Q, Xu M X, Wang L. *Chin J Catal*), 2008, **29**: 1159
11 Jiang J, Li R, Wang H L, Zheng Y F, Chen H N, Ma J T. *Catal Lett*, 2008, **120**: 221
12 Chou K S, Lee S J. *Colloid Surf A*, 2009, **336**: 23
13 Rane K S, Verenkar V M S, Pednekar R M, Sawant P Y. *J Mater Sci Mater Electron*, 1999, **10**: 121
14 Basak S, Rane K S, Biswas P. *Chem Mater*, 2008, **20**: 4906

15 Shi F, Tse M K, Pohl M M, Radnik J, Brückner A, Zhang S M, Beller M. *J Mol Catal A*, 2008, **292**: 28
16 Zhang Y, Li Z, Sun W, Xia C G. *Catal Commun*, 2008, **10**: 237
17 Zhang Y, Xia C G. *Appl Catal A*, 2009, **366**: 141
18 Liu H Q, Liang M H, Xiao C, Zheng N, Feng X H, Liu Y, Xie J L, Wang Y. *J Mol Catal A*, 2009, **308**: 79
19 Oliveira R L, Kiyohara P K, Rossi L M. *Green Chem*, 2010, **12**: 144
20 Qi B, Lu X H, Zhou D, Xia Q H, Tang Z R, Fang S Y, Pang T, Dong Y L. *J Mol Catal A*, 2010, **322**: 73
21 Wilson K, Hardacre C, Lee A F, Montero J M, Shellard L. *Green Chem*, 2008, **10**: 654
22 李渊, 赵新强, 王延吉. 催化学报(Li Y, Zhao X Q, Wang Y J. *Chin J Catal*), 2004, **25**: 633
23 Macala G S, Matson T D, Johnson C L, Lewis R S, Iretskii A V, Ford P C. *ChemSusChem*, 2009, **2**: 215
24 Calvino-Casilda V, Martin-Aranda R M, Lopez-Peinado A J, Sobczak I, Ziolek M. *Catal Today*, 2009, **142**: 278
25 Sharma S K, Parikh P A, Jasra R V. *J Mol Catal A*, 2010, **317**: 27
26 Teng X W, Black D, Watkins N J, Gao Y L, Yang H. *Nano Lett*, 2003, **3**: 261
27 Liu X M, Li Y S. *Mater Sci Eng C*, 2009, **29**: 1128
28 Pereira C, Pereira A M, Quaresma P, Tavares P B, Pereira E, Araújo J P, Freire C. *Dalton Trans*, 2010, **39**: 2842
29 Lutzenkirchen-Hecht D, Strehblow H H. *Surf Interface Anal*, 2009, **41**: 820
30 You X F, Chen F, Zhang J L, Anpo M. *Catal Lett*, 2005, **102**: 247
31 Sangpour P, Babapour A, Akhavana O, Moshfegh A Z. *Surf Interface Anal*, 2009, **41**: 157
32 Mackova A, Malinsky P, Bocan J, Svorcik V, Pavlik J, Stryhal Z, Sajdl P. *Phys Stat Sol C*, 2008, **5**: 964
33 Zhang D H, Li H B, Li G D, Chen J S. *Dalton Trans*, 2009, **47**: 10527
34 Schnippering M, Carrara M, Foelske A, Kötz R, Fermín D J. *Phys Chem Chem Phys*, 2007, **9**: 725
35 Miyakoshi A, Ueno A, Ichikawa M. *Appl Catal A*, 2001, **219**: 249
36 Hope G A, Woods R, Buckley A N, White J M, McLean J. *Inorg Chim Acta*, 2010, **363**: 935
37 Schubert M M, Hackenberg S, Van Veen A C, Muhler M, Plzak V, Behm R J. *J Catal*, 2001, **197**: 113
38 Liu H C, Kozlov A I, Kozlova A P, Shido T, Iwasawa Y. *Phys Chem Chem Phys*, 1999, **1**: 2851
39 Yang Y, Guan J Q, Qiu P P, Kan Q B. *Transition Met Chem*, 2010, **35**: 263
40 Lu X N, Yuan Y Z. *Appl Catal A*, 2009, **365**: 180